

# Functional and Evolutionary Integration of a Fungal Gene With a Bacterial Operon

Liang Sun,<sup>1,2</sup> Kyle T. David,<sup>3</sup> John F. Wolters,<sup>1,2</sup> Steven D. Karlen,<sup>1</sup> Carla Gonçalves ,<sup>2,3,4</sup> Dana A. Opulente ,<sup>1,2,5</sup> Abigail Leavitt LaBella,<sup>3,6</sup> Marizeth Groenewald,<sup>7</sup> Xiaofan Zhou ,<sup>3,8</sup> Xing-Xing Shen ,<sup>3,9</sup> Antonis Rokas ,<sup>3</sup> and Chris Todd Hittinger ,<sup>1,2,\*</sup>

<sup>1</sup>DOE Great Lakes Bioenergy Research Center, University of Wisconsin-Madison, Madison, WI 53726, USA

<sup>2</sup>Laboratory of Genetics, Center for Genomic Science Innovation, Wisconsin Energy Institute, J. F. Crow Institute for the Study of Evolution, University of Wisconsin-Madison, Madison, WI 53726, USA

<sup>3</sup>Evolutionary Studies Initiative and Department of Biological Sciences, Vanderbilt University, Nashville, TN 37235, USA

<sup>4</sup>UCIBIO, Department of Life Sciences, NOVA School of Science and Technology, Universidade NOVA de Lisboa, Caparica, Portugal

<sup>5</sup>Biology Department, Villanova University, Villanova, PA 19085, USA

<sup>6</sup>Department of Bioinformatics and Genomics, University of North Carolina at Charlotte, Charlotte, NC 28223, USA

<sup>7</sup>Westerdijk Fungal Biodiversity Institute, 3584 CT Utrecht, The Netherlands

<sup>8</sup>Guangdong Province Key Laboratory of Microbial Signals and Disease Control, Integrative Microbiology Research Center, South China Agricultural University, Guangzhou 510642, China

<sup>9</sup>College of Agriculture and Biotechnology and Centre for Evolutionary & Organismal Biology, Zhejiang University, Hangzhou 310058, China

**\*Corresponding author:** E-mail: cthittinger@wisc.edu.

**Associate editor:** Jeffrey Townsend

## Abstract

Siderophores are crucial for iron-scavenging in microorganisms. While many yeasts can uptake siderophores produced by other organisms, they are typically unable to synthesize siderophores themselves. In contrast, *Wickerhamiella/Starmerella* (W/S) clade yeasts gained the capacity to make the siderophore enterobactin following the remarkable horizontal acquisition of a bacterial operon enabling enterobactin synthesis. Yet, how these yeasts absorb the iron bound by enterobactin remains unresolved. Here, we demonstrate that *Enb1* is the key enterobactin importer in the W/S-clade species *Starmerella bombicola*. Through phylogenomic analyses, we show that *ENB1* is present in all W/S clade yeast species that retained the *enterobactin* biosynthetic genes. Conversely, it is absent in species that lost the *ent* genes, except for *Starmerella stellata*, making this species the only cheater in the W/S clade that can utilize enterobactin without producing it. Through phylogenetic analyses, we infer that *ENB1* is a fungal gene that likely existed in the W/S clade prior to the acquisition of the *ent* genes and subsequently experienced multiple gene losses and duplications. Through phylogenetic topology tests, we show that *ENB1* likely underwent horizontal gene transfer from an ancient W/S clade yeast to the order Saccharomycetales, which includes the model yeast *Saccharomyces cerevisiae*, followed by extensive secondary losses. Taken together, these results suggest that the fungal *ENB1* and bacterial *ent* genes were cooperatively integrated into a functional unit within the W/S clade that enabled adaptation to iron-limited environments. This integrated fungal-bacterial circuit and its dynamic evolution determine the extant distribution of yeast enterobactin producers and cheaters.

**Key words:** enterobactin, fungal, bacterial, operon, siderophore, iron.

## Introduction

Most organisms on earth require iron as a redox mediator that is key to numerous biological processes, including respiration; protection from reactive oxygen species; photosynthesis; and the biosynthesis of amino acids, lipids,

deoxyribonucleotides, and sterols. Although iron is abundant in the crust of Earth, its availability to living organisms is generally low. This poor bioavailability occurs because iron exists mainly in its oxidized ferric ( $Fe^{3+}$ ) state, which is largely insoluble in water in neutral and basic pH

**Received:** November 21, 2023. **Revised:** February 19, 2024. **Accepted:** February 21, 2024

© The Author(s) 2024. Published by Oxford University Press on behalf of Society for Molecular Biology and Evolution.

This is an Open Access article distributed under the terms of the Creative Commons Attribution-NonCommercial License (<https://creativecommons.org/licenses/by-nc/4.0/>), which permits non-commercial re-use, distribution, and reproduction in any medium, provided the original work is properly cited. For commercial re-use, please contact [reprints@oup.com](mailto:reprints@oup.com) for reprints and translation rights for reprints. All other permissions can be obtained through our RightsLink service via the Permissions link on the article page on our site—for further information please contact [journals.permissions@oup.com](mailto:journals.permissions@oup.com).

**Open Access**

environments. To circumvent iron shortage, microorganisms have evolved the capacity to scavenge iron from environmental stocks by secreting and taking up siderophores, a chemically diverse group of secondary metabolites that bind to  $\text{Fe}^{3+}$  with very high affinity and specificity (Haas et al. 2008; Kramer et al. 2020). These siderophore-mediated iron acquisition systems require active synthesis and secretion of siderophores in iron-free form, as well as specific transporter mechanisms to recognize and selectively take up the  $\text{Fe}^{3+}$ -siderophore complex.

In contrast to most bacteria and filamentous fungi, yeasts of the subphylum Saccharomycotina (hereafter, yeasts) are generally unable to synthesize siderophores with a few exceptions, such as *Kluyveromyces lactis*, which produces pulcherrimin (Krause et al. 2018). The model yeast *Saccharomyces cerevisiae*, however, can utilize iron bound to various structurally distinct siderophores produced by other microbial species through 2 distinct systems (Yun et al. 2001). One system depends on the FRE gene family, which encodes plasma membrane reductases (Fre1, Fre2, or Fre3) that reduce and dissociate iron from siderophores at the cell surface; iron is then translocated through the plasma membrane by the high-affinity ferrous iron ( $\text{Fe}^{2+}$ ) transporter complex (Ftr1 and Fet3) (Stearman et al. 1996). Another system depends on four siderophore transporters of the major facilitator superfamily (MFS) that are distinct in substrate specificity and named Arn1, Arn2, Sit1 (also known as Arn3), and Enb1 (also known as Arn4) (Lesuisse et al. 1998; Heymann et al. 1999; Heymann et al. 2000a; Heymann et al. 2000b). This system allows a  $\text{Fe}^{3+}$ -siderophore complex to enter the cells prior to any reduction step with high affinity and high specificity. Among these siderophore transporters, Enb1 is highly specific to the siderophore enterobactin and has previously only been reported in yeasts belonging to the genus *Saccharomyces* (Heymann et al. 2000b), whereas Sit1 transporters, which recognize a wide variety of siderophores, are abundant across the yeast phylogeny (Dias and Sá-Correia 2013). From an ecological and evolutionary perspective, siderophores can be shared between cells as public goods, and their production typically represents a form of cooperation (Julou et al. 2013; Weigert and Kümmerli 2017). However, yeasts with siderophore transporters can act as cheaters and exploit the benefits of siderophore production without paying the cost of synthesis and, thus, may outcompete the producers to a certain extent (Griffin et al. 2004; Dumas and Kümmerli 2012). The potential fitness benefits of being a cheater may have driven the evolution of siderophore transporter diversity in yeasts. While the biochemical properties of siderophore transporters have been examined by a wealth of studies in *S. cerevisiae* and other model yeasts (Yun et al. 2000; Ardon et al. 2001; Heymann et al. 2002), their evolutionary origins are largely unknown.

The exponentially rising amount of genomic sequence data has made yeast comparative genomics a powerful tool to explore the genetic bases and evolutionary histories of important traits (Butler et al. 2004; Hittinger and Carroll 2007; Marcet-Houben and Gabaldón 2015; Vakirlis et al.

2016; Gonçalves and Gonçalves 2019; Krause and Hittinger 2022). One of the most striking evolutionary events brought to light by comparative genomics is the horizontal operon transfer (HOT) of an *enterobactin* biosynthesis pathway from an ancient bacterium in the order Enterobacteriales into the *Wickerhamiella/Starmerella* (W/S) clade of yeasts (Kominek et al. 2019). All the *ent* genes required for enterobactin biosynthesis were maintained and functionally expressed in at least some of the yeast species examined, which constituted a newly discovered and surprising group of enterobactin producers. However, genes encoding bacterial ATP binding cassette (ABC) transporters for enterobactin uptake were not found in these yeasts. The capacity to lock iron away from competitors would be counterproductive if the producer species were unable to utilize the iron bound to enterobactin, which suggests the presence of one or more alternative transporter mechanisms in the W/S clade yeasts.

Besides the *ent* HOT, the W/S clade yeasts were reported to have acquired many genes from bacteria through independent horizontal gene transfer (HGT) events (Gonçalves and Gonçalves 2019; Gonçalves et al. 2018). Most species of the W/S clade are ecologically associated with flowers and floricolous insects, where stable bacterial and eukaryotic communities coexist (Gilliam 1997; Lachance et al. 2001; Gonçalves et al. 2020). One species in the clade, *Starmerella bombicola*, has been applied for the industrial production of biosurfactants called sophorolipids and has been recently used as an engineering model to study the evolution of yeast metabolism due to its genetic tractability and acquisition of foreign genes via HGT (De Graeve et al. 2018).

Siderophore-mediated iron uptake is crucial for fungal iron homeostasis and virulence, but it has rarely been studied in yeasts other than *S. cerevisiae* and the opportunistic pathogen *Candida albicans* (Haas et al. 2008). Here, we investigate iron transport mechanisms using the enterobactin-producing yeast *St. bombicola* as a model for targeted gene disruption and show that this species uses the Enb1 transporter for the uptake of enterobactin-bound iron. Through phylogenomic analyses, we show that *ENB1* is a fungal gene that was likely present in the most recent common ancestor (MRCA) of the Dikarya, the fungal clade that contains the phyla Basidiomycota and Ascomycota. This fungal gene was then functionally integrated with the horizontally acquired bacterial *ent* operon in the W/S-clade yeasts as an adaptation to varying iron availability. Finally, we infer that a horizontal transfer of the *ENB1* gene from an ancestor of the W/S clade (order Dipodascales) to an ancestor of the order Saccharomycetales (which includes *S. cerevisiae*), along with multiple independent gene duplications and losses, shaped the patchy phylogenetic distribution of enterobactin cheaters in yeasts. This study highlights the intriguing interplay between fungal and bacterial genes, which formed a functional unit in some yeasts to produce a valuable resource, and later separated through dynamic evolution as cheaters arose to exploit that resource.

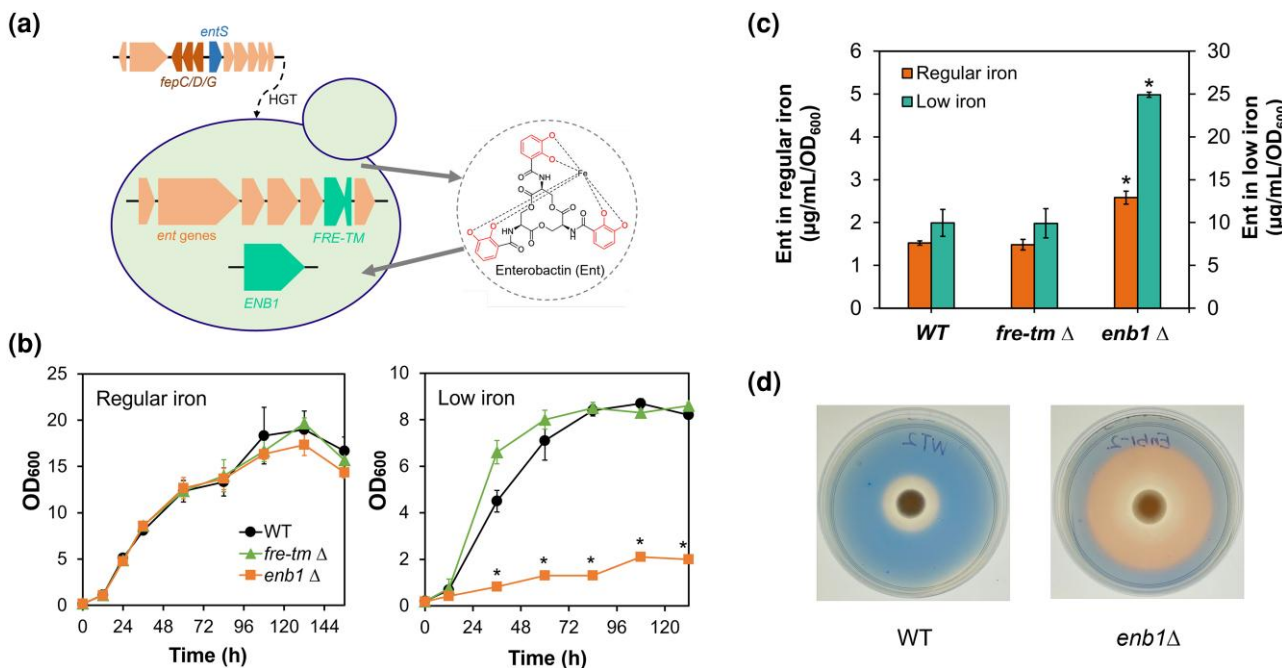


**Fig. 1.** Enb1 is the key transporter mediating the uptake of enterobactin-bound iron in *St. bombicola*. Genes related to enterobactin biosynthesis and candidate genes for transport are native fungal genes or underwent horizontal gene transfer (HGT) from a bacterial operon (a). Growth of *St. bombicola* WT and mutants in regular- and low-iron conditions (b). The minimal growth of the *enb1* $\Delta$  strain in low-iron medium could be attributed to intracellular iron storage in vacuoles and other compartments during preculturing (Raguzzi et al. 1988) or reductive transport of enterobactin-bound iron with low affinity (Lesuisse et al. 2001). Extracellular enterobactin accumulation of *St. bombicola* mutants (c). O-CAS assay of the WT and *enb1* $\Delta$  mutants; iron sequestration converts the dark blue color to light orange (d). Data are presented as mean values and standard deviations of three independent biological replicates. Statistical significance of the differences between the *enb1* $\Delta$ , *fre-tm* $\Delta$ , and WT strains was evaluated by Student's *t*-test. \*, *P*-value < 0.001.

## Results and Discussion

**Enb1 Imports Enterobactin in *Stammerella bombicola***  
 While the HOT event and the subsequent genetic adaptations enabling bacterial gene expression and enterobactin synthesis in the W/S-clade yeasts are well-documented (Kominek et al. 2019), the mechanism by which these yeasts uptake the iron bound by enterobactin remains unknown. In the model bacterium *Escherichia coli*, the Fe<sup>3+</sup>-enterobactin complex is first translocated into the periplasm by the outer-membrane siderophore receptor FepA; it is then transported into the cytoplasm via the ABC transporter encoded by three genes: *fepC*, *fepD*, and *fepG*, which are parts of the *E. coli* *ent* operon (Usher et al. 2001; Raymond et al. 2003). However, neither *fepA*, *fepC*, *fepD*, nor *fepG* was found in the genomes of any W/S-clade yeasts, suggesting the presence of one or more alternative transport mechanisms.

We examined the possible mechanisms by which W/S-clade yeasts utilize enterobactin-bound iron using *St. bombicola* as a genetically tractable model species. Functionally related genes are often located in genomic proximity, even in eukaryotes (Hurst et al. 2004). The intercalation of genes encoding a eukaryotic ferric reductase (Fre) and an uncharacterized transmembrane protein (Tm) between 2 *ent* genes in a subset of the W/S-clade yeasts suggested a possible role in reductive uptake for

this *FRE-TM* gene pair (Fig. 1a). We also identified a homolog of the *S. cerevisiae* *ENB1* (*ScENB1*) in *St. bombicola* with 52% amino-acid sequence identity and 96% coverage, which suggested the possibility that its function might be conserved as well. To determine which, if any, of these candidate genes were involved in the utilization of enterobactin-bound iron, we engineered two *St. bombicola* mutants by deleting either the *ScENB1* homolog (*enb1* $\Delta$ ) or the *FRE-TM* (*fre-tm* $\Delta$ ) gene cluster and compared their growth to the wildtype (WT) strain in both regular and low-iron media. The *fre-tm* $\Delta$  mutant exhibited comparable growth patterns to the WT in both media (Fig. 1b), suggesting the *FRE-TM* gene pair is not essential for iron acquisition or could be functionally redundant with other ferric reductase genes, including homologs of *FRE1-FRE8* (Yun et al. 2001). Although it grew normally with regular-iron concentrations, the *enb1* $\Delta$  strain showed minimal growth in low-iron conditions (Fig. 1b). This result implies that the Enb1 homolog plays a crucial role in iron uptake in iron-limited conditions.

To delve into the function of the Enb1 homolog, we measured the levels of extracellular enterobactin. We found that all three strains produced substantially higher amounts of enterobactin in low-iron medium compared to regular medium (6.5 to 9.6-fold increase) (Fig. 1c). This result indicates that enterobactin biosynthesis in *St. bombicola* increases under conditions of iron scarcity and might have evolved as an integral part of the

regulatory network governing iron hemostasis. Moreover, the *fre-tm1* strain amassed similar levels of enterobactin as the WT in both culturing conditions, whereas cells of the *enb1Δ* strain accumulated 1.7-fold and 2.5-fold more enterobactin than the WT in regular medium and low-iron medium, respectively. An orthogonal colorimetric assay also showed a notably stronger enterobactin signal from the *enb1Δ* strain as compared to the WT strain (Fig. 1d), which suggests that the mutant experiences severe iron starvation in low-iron conditions because it cannot effectively import enterobactin. Thus, we conclude that the *ENB1* homolog encodes a functional Enb1 transporter that is required for normal uptake of enterobactin-bound iron in *St. bombicola*.

Interestingly, disruption of neither *ENB1* nor *FRE-TM* noticeably affected the export of enterobactin. In *E. coli*, *entS*, as part of the *ent* operon, encodes the primary enterobactin exporter, which, together with the outer-membrane channel TolC, mediates the secretion of enterobactin (Furrer et al. 2002). Since no homolog of *entS* could be identified in *St. bombicola* and other W/S-clade yeasts (Kominek et al. 2019), how the enterobactin synthesized in the cells is secreted to the medium remains an unanswered question.

### The Origin of *ENB1*

To determine whether *ENB1* was horizontally acquired by the W/S-clade yeasts from bacteria like the *ent* genes, we performed Basic Local Alignment Search Tool protein (BLASTp) searches against the National Center for Biotechnology Information (NCBI) non-redundant sequences (nr) database using the amino-acid sequence of *St. bombicola* Enb1 (*StbEnb1*) as the query. Proteins from the Saccharomycetales, including *ScEnb1*, were retrieved with *E*-values equal to or lower than 5e-132, above which point proteins from filamentous fungi started to be recovered (supplementary dataset S1-1, Supplementary Material online). The *E*-values obtained from some filamentous fungi hits were as low as 2e-117, suggesting strong sequence similarity with the *StbEnb1*. Among the top 2,626 BLASTp hits recovered using an *E*-value cutoff of e-60, only a few were from archaea or bacteria, while all the others were fungal proteins (supplementary dataset S1-2, Supplementary Material online). According to the maximum likelihood (ML) phylogeny constructed with these top hits (supplementary fig. S1, Supplementary Material online), *StbEnb1* and its close homologs from the Saccharomycetales clustered monophyletically on a long branch with 100% bootstrap support, whereas the proteins from archaea and bacteria scattered across the larger gene tree on distant branches. Hence, we conclude that closely related Enb1 homologs are only found in fungi, and the *StbENB1* gene is unlikely to have been acquired horizontally from bacteria.

The high sequence similarity of *StbEnb1* to proteins from filamentous fungi inspired us to examine the evolutionary history of Enb1 in the kingdom of Fungi. For this purpose,

we conducted a hidden Markov model (HMMER) scan for Enb1 homologs against a dataset containing 1,644 published fungal genomes (Li et al. 2021) using the aligned sequences of *ScEnb1* and *StbEnb1* as queries; we obtained 1,061 protein sequences by employing a bit-score cutoff of 300 and a *E*-value cutoff of 0.05 (supplementary dataset S2, Supplementary Material online). The resulting proteins were exclusively from the Dikarya; the vast majority of them were recovered from the subphyla Saccharomycotina (491) and Pezizomycotina (553), while only 17 of them were from the subphyla Agaricomycotina, Walleiomycotina, and Taphrinomycotina. After accounting for putative gene duplication events that gave rise to distantly related paralogs (e.g. genes encoding *Arn1*, *Arn2*, and *Sit1*), the ML phylogenetic tree constructed using the 1,061 protein sequences (supplementary fig. S2, Supplementary Material online) was generally consistent with the reported genome-scale species phylogeny (Li et al. 2021). Notably, *ScEnb1* and *StbEnb1*, as well as Enb1 homologs from many yeasts belonging to the W/S clade and the order Saccharomycetales, formed a monophyletic group with 12 proteins from diverse fungi at 98% bootstrap confidence. The 12 closest relatives of yeast Enb1 were recovered from species that were scattered sparsely, but widely, in the Dikarya across the subphyla Pezizomycotina, Agaricomycotina, Walleiomycotina, and Taphrinomycotina. Since this sparse clade roughly matched the species phylogeny, we propose that it comprises the extant Enb1 orthologs. Under this model, *ENB1* was likely present in the MRCA of the Dikarya, while its sparse and dispersed distribution is likely due to extensive losses in the various lineages.

Interestingly, the non-Saccharomycotina fungal species encoding Enb1 are either known plant pathogens, including *Eutypa lata*, *Rhizoctonia solani*, *Passalora fulva*, and *Ceratobasidium theobromae* (Thomma et al. 2005; Ajayi-Oyetunde and Bradley 2018; Ali et al. 2019; Lolas et al. 2020); or they can exhibit yeast-like growth, including three fission yeasts (*Schizosaccharomyces japonicus*, *Schizosaccharomyces octosporus*, and *Schizosaccharomyces cryophilus*), three dimorphic fungi (*Zymoseptoria brevis*, *Zymoseptoria ardabilliae*, and *Prillingera fragicola*) (Quaedvlieg et al. 2011; Takashima et al. 2019), and a basidiomycetous yeast (*Apotrichum gamsii*) (James et al. 2016). This unusual phylogenetic distribution suggests a potential role of Enb1 in the evolution of fungal virulence and unicellular yeast growth, which is consistent with the previous finding that siderophore-mediated iron uptake is crucial for fungal iron homeostasis and virulence (Haas et al. 2008).

### Horizontal Gene Transfer of *ENB1* Within Yeasts

The presence of *ENB1* in *St. bombicola* and *S. cerevisiae*, which belong to two distantly related orders that diverged over 300 million years ago (Shen et al. 2018; Groenewald et al. 2023), prompted us to more thoroughly investigate its species distribution within the subphylum Saccharomycotina. We performed a HMMER search against

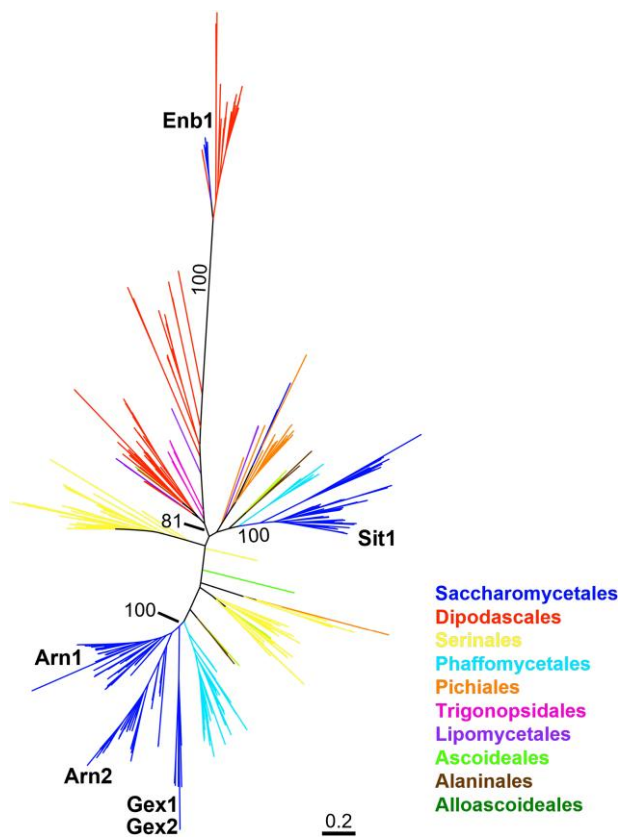


**Fig. 2.** ML phylogeny of Enb1 homologs, including paralogs, from the yeast subphylum Saccharomycotina using an amino-acid sequence alignment. Branch values shown are the percentages of branch support out of 1,000 bootstrap replicates. The 4 Arn family siderophore transporters (Arn1, Arn2, Sit1, and Enb1) and 2 glutathione exchangers (Gex1 and Gex2) from *S. cerevisiae* are labeled in the tree, which share the MFS domain based on InterProScan (Paysan-Lafosse et al. 2023). Yeast major clades are colored according to their taxonomic assignment to an order of Saccharomycotina (Groenewald et al. 2023). *Supplementary fig. S3, Supplementary Material* online shows a midpoint-rooted version of the same ML phylogeny; this rooting supports the conclusion that Enb1 is monophyletic.

345 publicly available yeast genomes (Shen et al. 2018; Kominek et al. 2019) for Enb1 homologs using aligned sequences of Enb1 from *S. cerevisiae* (ScEnb1) and *St. bombicola* (StbEnb1) as the query. In addition to ScEnb1 and StbEnb1, 32 proteins, exclusively from the order Saccharomycetales and W/S clade of yeasts, were retrieved up to *E*-value of 3.9e-170 and bit-score of 565.5, after which point the *E*-value ramped up and hit score dropped drastically (Dataset S3). All 34 closely related Enb1 homologs clustered monophyletically on a very long branch with 100% bootstrap support in the ML phylogeny (Fig. 2 and *supplementary fig. S3, Supplementary Material* online). Besides Enb1, we recovered the other 3 siderophore transporters, Arn1, Arn2, and Sit1, as well as the glutathione exchanger Gex1 and its paralog Gex2 (Dhaoui et al. 2011) from *S. cerevisiae*. Consistent with previous observations (Diffels et al. 2006; Dias and Sá-Correia 2013), *S. cerevisiae* Arn1, Arn2, Gex1, and Gex2, as well as all their homologs from other

Saccharomycetales species, formed a single clade in the tree with 100% bootstrap support.

From these searches, we discovered clear ENB1 orthologs in species from the genera *Saccharomyces*, *Torulaspora*, and *Lachancea*. Surprisingly, these ENB1 orthologs from the order Saccharomycetales were nested within those of the W/S clade (Fig. 2 and *supplementary fig. S3, Supplementary Material* online), which suggests the possibility of a HGT event from the W/S clade in the order Dipodascles to the order Saccharomycetales. This model is consistent with the fact that previously known ENB1 homologs were identified exclusively in the subtelomeric regions of yeasts belonging to the genus *Saccharomyces* (Dias and Sá-Correia 2013), which constitute a favorable chromosomal location for the acquisition of foreign genes (Kellis et al. 2003; Novo et al. 2009). To better illuminate the evolution of Enb1 within yeasts, we identified three more Enb1 homologs from *Wickerhamiella shivajii* and *Starmerella stellata*, whose genomes were recently published (Opulente et al. 2023). Using ML, we carefully examined the phylogenetic relationships between the 37 yeast Enb1-like protein sequences, as well as the 7 closest relatives of Enb1 from fungal outgroups. As expected, the yeast Enb1-like transporters formed a monophyletic clade with 100% bootstrap support (Fig. 3a, *supplementary fig. S2, Supplementary Material* online). However, there were at least 3 instances where the Enb1 tree did not recover the expected phylogenetic relationships between yeast taxa (Figs. 3a and 4). Most notably, Enb1 homologs from the Saccharomycetales were nested within the W/S clade and indeed were sister to the distantly related species *St. stellata* with 96% bootstrap support. This observation suggests the acquisition via HGT of an ENB1 gene by an ancient Saccharomycetales from an ancestor of W/S clade yeasts. To test this hypothesis, we performed topology tests where we compared the likelihood of the ML-supported (unconstrained) topology against the likelihood of an alternative constrained topology that enforced the reciprocal monophyly of the Saccharomycetales- and W/S-clade homologs (Fig. 3b). Both weighted Shimodaira–Hasegawa (wSH) and approximately unbiased (AU) tests significantly rejected the null model of vertical inheritance and instead supported HGT (Fig. 3c).

Second, the *St. stellata* Enb1 homolog did not associate as expected with other *Starmerella* branches of the tree in the Enb1 phylogeny (*supplementary fig. S4A, Supplementary Material* online). Instead, *St. stellata* Enb1 formed a monophyletic clade with the Saccharomycetales, *Wickerhamiella pararugosa*, and *W. shivajii* homologs. This topology suggests another possible HGT event from this *Wickerhamiella* lineage into an ancestor of *St. stellata*. To test for additional HGT events between *Wickerhamiella* and *Starmerella*, we performed a series of topology tests. First, we enforced the placement of *St. stellata* Enb1 either as an outgroup of the *Starmerella* Enb1 clade (Constrained Topology 2, *supplementary fig. S4B, Supplementary Material* online) or to its exact location in the species phylogeny (Constrained

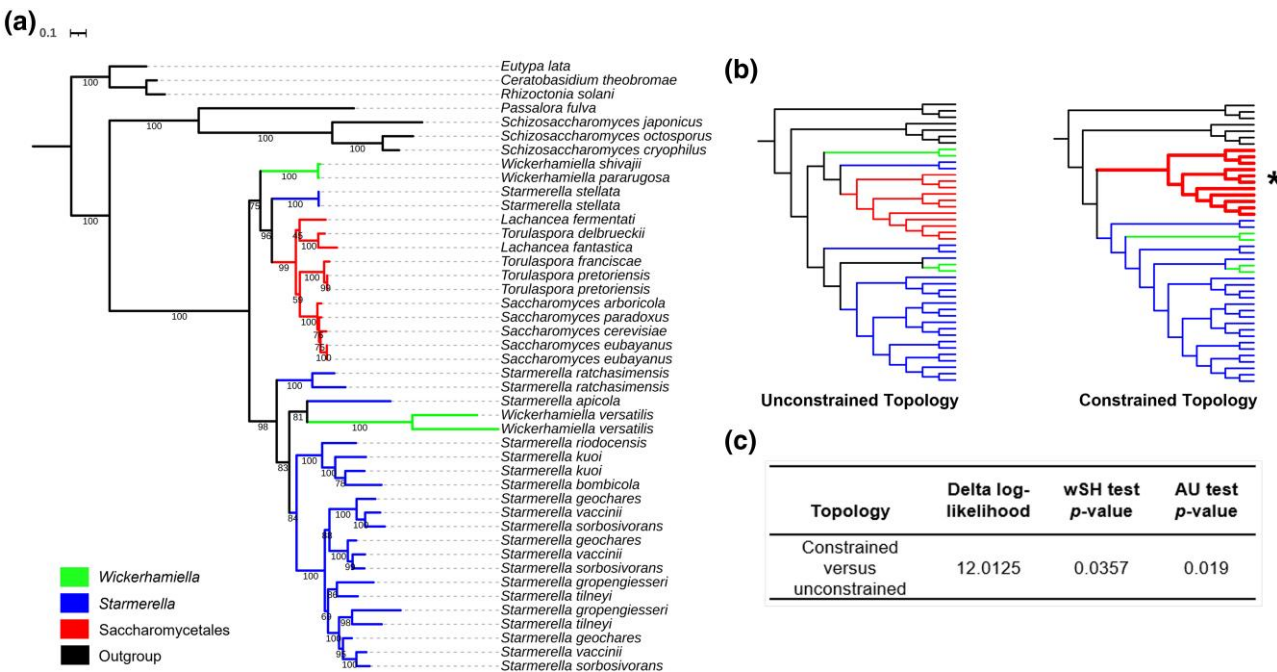


**Fig. 3.** Evidence for HGT of *ENB1* in yeasts. ML phylogeny of the fungal *Enb1* protein sequences most closely related to *Saccharomycotina* *Enb1* (a), which are a clade from the full analyses shown in [supplementary fig. S1, Supplementary Material](#) online. The 7 closest relatives of *Enb1* proteins from filamentous fungi were chosen as outgroups. Branch values shown are the percentages of branch support out of 1,000 bootstrap replicates. Branches are colored to represent species from the genera *Wickerhamiella*, *Stamerella*, order *Saccharomycetales*, and outgroup lineages. Branches with the same species name occur because some genomes encode multiple copies of *Enb1*. The simplified topologies of the unconstrained and constrained gene trees are shown in (b). Branches repositioned in the constrained topology are highlighted with wider lines and denoted with (\*). The wSH (weighted Shimodaira–Hasegawa) and AU topology test results are shown in (c). P-values of the wSH test and the AU test were both lower than the statistical significance threshold of 0.05.

Topology 3, [supplementary fig. S4B, Supplementary Material](#) online). The wSH and AU tests of Constrained Topology 3 robustly rejected the null model of vertical inheritance, while the same tests of Constrained Topology 2 did not reject the null model ([supplementary fig. S4C, Supplementary Material](#) online). Since Constrained Topology 3 incorporates additional incongruences between the gene and species phylogenies, we conclude that HGT from an ancient *Wickerhamiella* into an ancestor of *St. stellata* is one of many evolutionary models that are consistent with the data, including more complex scenarios involving multiple HGT events, cryptic gene duplication, or incomplete lineage sorting within the W/S clade. Additionally, the topology tests did not significantly support a possible HGT associated with the *Wickerhamiella versatilis* *Enb1* (Constrained Topology 1, [supplementary fig. S4B and S4C, Supplementary Material](#) online). Given the evolutionary distances involved, we conclude that *ENB1* has experienced a complex history in some W/S-clade lineages, including the lineage leading to *St. stellata*. We further conclude that one of these ancient W/S lineages likely acted as the donor of the *Saccharomycetales* *ENB1*.

### Duplications and Losses of *ENB1* and Its Functional Integration With a Bacterial Operon

To get more insight into the evolutionary mechanisms leading to the distribution of *ENB1* orthologs in yeasts,

we mapped its presence, absence, and copy numbers onto a genome-scale species phylogeny inferred in a recent publication ([Opulente et al. 2023](#)) (Fig. 4). Given its broad distribution in the clade, *ENB1* was almost certainly present in the MRCA of the W/S clade. It could have been acquired from other fungi by HGT, or *ENB1* could have been present in the MRCA of *Saccharomycotina* and then lost in all other known yeast lineages (at least 9 independent losses by maximum parsimony). The *St. bombicola* *enb1Δ* mutant phenotype (Fig. 1) indicates that expression of an *Enb1* transporter is essential for normal uptake of iron bound to enterobactin. Thus, *ENB1* would convey a selective advantage in iron-limited environments where enterobactin is present, including enterobactin made by other microbes, but especially for organisms making their own enterobactin. Therefore, we hypothesize that the *ENB1* gene was actively expressed in the MRCA of the W/S-clade yeasts prior to the HOT event that introduced the *ent* operon into yeasts. Under this scenario, the *fepC/D/G* genes from the operon, which would have encoded the bacterial ABC-type enterobactin transporters, could have been lost easily due to functional redundancy with fungal *ENB1*.

The phylogenetic distribution of *ENB1* copy numbers and inference by maximum parsimony suggest at least two duplication events in the W/S clade: one that occurred before the divergence of *W. versatilis*, *Wickerhamiella domercqiae*,

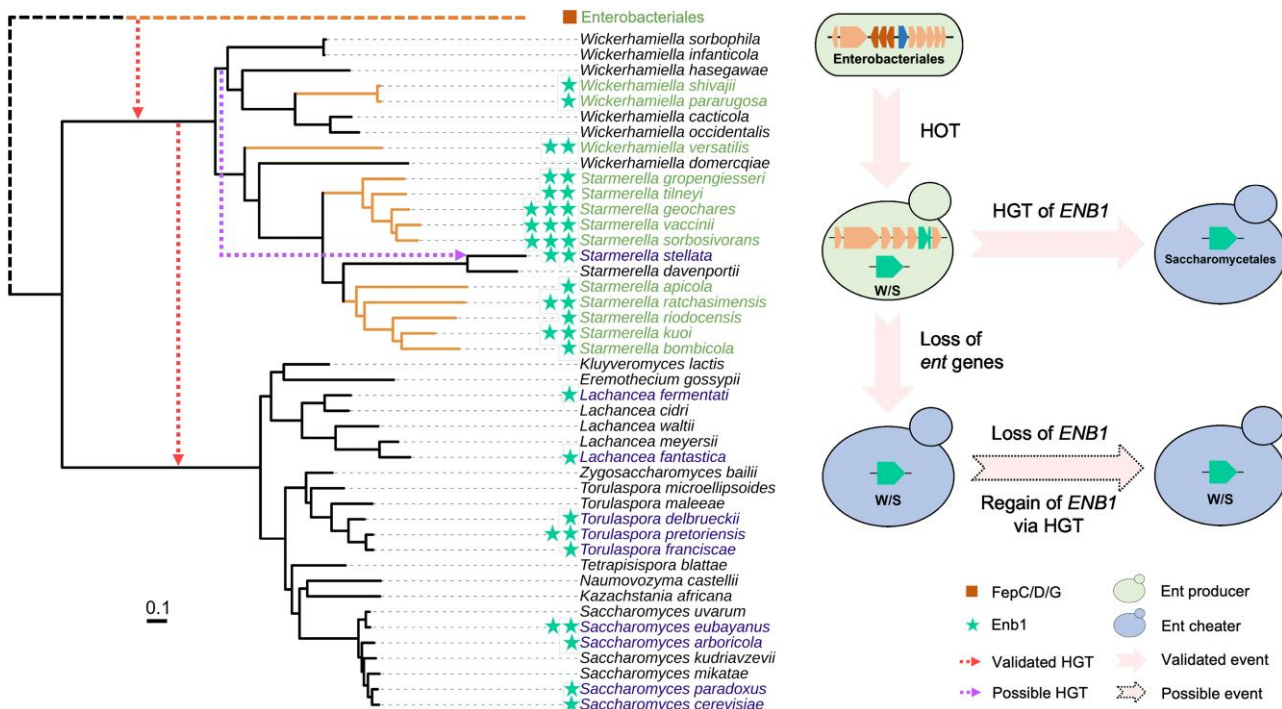


**Fig. 4.** Evolution of the fungal enterobactin transporter encoded by *ENB1* and its functional integration with the bacterial *ent* operon in yeasts. The genome-scale species phylogeny was adapted from a recent publication (Opulente et al. 2023) by pruning irrelevant branches of the phylogeny of 1,154 yeasts using iTOL (Interactive Tree of Life) v5 (Letunic and Bork 2021). Branches colored in orange represent the presence of *ent* genes. Dashed arrows denote validated possible horizontal gene transfer (HGT) events, according to the color in the key. The square represents genes encoding the Enterobacteriales FepC/D/G ABC-type enterobactin transporter. Stars represent the number of genes encoding fungal Enb1 transporters. Branch names in green represent enterobactin producers harboring both *ENB1* and *ent* genes. Branch names in blue represent enterobactin cheaters harboring only genes encoding the Enb1 transporter. Species with names in black have neither *ENB1* nor *ent* genes. Gene icons are colored as in Fig. 1.

and the genus *Starmerella*; and a second that occurred in the last common ancestor of *Starmerella geochares*, *Starmerella vaccinii*, and *Starmerella sorbosivorans*. This model is generally consistent with the Enb1 protein tree (Fig. 3a). Additionally, maximum parsimony suggests multiple loss events occurred both prior to and following the duplications, leading to reduced copy numbers of *ENB1* absence in some W/S-clade yeasts. According to the branch lengths in the protein tree (Fig. 3a), the protein sequences of Enb1 in the W/S clade yeasts are generally more divergent than those in the Saccharomycetales, indicating faster evolution of the W/S clade Enb1. To estimate patterns of selection for the *ENB1* duplicated copies, we further analyzed the ratio of nonsynonymous to synonymous substitution rates (*dN/dS*) across the phylogeny of Saccharomycotina Enb1 (supplementary fig. S5 and dataset S7, Supplementary Material online). All valid *dN/dS* values (those with *dS*  $\geq 0.005$ ) were significantly below 1, which suggests that *ENB1* genes in yeasts are under strong purifying selection and the duplicated copies are likely all functional (Kondrashov et al. 2002). Despite the notably rapid evolution of the two *ENB1* copies in *W. versatilis*, which appeared on long branches of the protein tree (supplementary fig. S5, Supplementary Material online), their *dN/dS* values still showed a clear signature of purifying selection. Disproportionate secretion and uptake of enterobactin

could also result in its extracellular accumulation, potentially reaching levels detrimental to the cells that produce it. We hypothesize that altering the copy number of the *ENB1* gene through duplications and losses might be an evolutionary strategy taken by the W/S-clade yeasts to balance the expression levels of the biosynthetic enzymes and the transporter, while adapting to new environments with different iron availability.

Copy number variation aside, the presence and absence of *ENB1* almost perfectly mirrors that of the *ent* genes encoding the enterobactin biosynthesis pathway within the W/S clade. Specifically, *ENB1* is present in all the W/S-clade yeasts that retained the *ent* genes, while it is absent in nearly all species that lost the *ent* genes, with *St. stellata* as the only exception. The correlation between the presence of the *ENB1* and *ent* genes is likely driven by the fact that the loss of *ENB1* would be deleterious to yeasts actively producing enterobactin because they would sequester iron that they could not import, a phenotype we observed in the *St. bombicola enb1Δ* mutant (Fig. 1b). The sole exception is *St. stellata*, which is the only W/S yeast that harbors the *ENB1* gene in the absence of *ent* genes, a genetic configuration known to create public goods cheaters in other siderophore systems (Wang et al. 2015; Krause et al. 2018). Regardless of whether *St. stellata* reacquired *ENB1* from an ancient *Wickerhamiella* species via HGT or not

(supplementary fig. S4, Supplementary Material online), it likely represents a reversion to the ancestral cheater state prior to the HOT event, either through simple loss of the *ent* operon or also through loss and subsequent regain of *ENB1*.

## Conclusions

Siderophores can readily bind iron, even in an iron-limited environment, thereby both reserving iron for producers and depriving iron from species that lack the matching transporter for uptake (Niehus et al. 2017; Schiessl et al. 2017). However, it has been repeatedly shown that non-producers possess conditional competitive advantages over the producers because they act as cheaters and exploit foreign siderophores without the cost of synthesis (Griffin et al. 2004; Jiricny et al. 2010; Dumas and Kümmerli 2012). The fact that the MRCA of the W/S clade was likely converted from a cheater for enterobactin into an enterobactin producer through HOT suggests that there were ecological and evolutionary circumstances where being a producer had an advantage over being a cheater. The HOT was proposed to have occurred in insect guts, which are believed to foster intense competition for iron among bacteria, yeasts, and the host itself (Barber and Elde 2015; Kominek et al. 2019). Yeasts with the capacity to produce their own enterobactin, which has an exceptionally high affinity for  $\text{Fe}^{3+}$  ( $K_f = 10^{51}$ ) (Carrano and Raymond 1979), may have been better positioned to outcompete nonproducers and species that produce different siderophores, especially in communities lacking enterobactin producers. Thus, the cooperative integration of the fungal *ENB1* gene and the bacterial *ent* genes as a functional unit for sequestering iron would have substantially contributed to the fitness of yeasts in highly competitive, iron-limited environments. After enterobactin-producing W/S-clade yeasts had begun to radiate, *ENB1* was horizontally transferred into an ancient lineage of Saccharomycetales (Fig. 3), which allowed many additional yeasts, including *S. cerevisiae* (Heymann et al. 2000b), to exploit the enterobactin produced by others. Several secondary losses of *ENB1* then led to its patchy distribution in the order Saccharomycetales. The retention of *ENB1* in cheaters may be associated with ecological niches where bacterial and fungal cohabitants produce enterobactin in response to iron scarcity. Conversely, the loss of *ENB1* may have occurred in yeasts dwelling in environments with relatively high iron availability or where enterobactin producers are absent.

Siderophore uptake has rarely been studied in nonconventional yeasts, but this study suggests it is subject to surprisingly complex eco-evolutionary dynamics. Here, we identified *Enb1* as the key transporter mediating the uptake of enterobactin-bound iron in *St. bombicola*, one of the extant W/S-clade yeasts that acquired a complete bacterial enterobactin biosynthesis pathway via an ancient HOT. Through phylogenomic analyses, we showed that the *ENB1* gene is of fungal origin and has a broad, but patchy, distribution in the Dikarya. Along with the horizontally

acquired bacterial operon, this fungal gene formed a mosaic functional unit that operates in many W/S-clade yeasts to scavenge iron from the environment. We also propose how cheaters arose through the secondary loss of the *ent* operon and/or HGT of *ENB1*. Multiple gene duplication and loss events punctuate the *ENB1* phylogeny and further suggest a dynamic eco-evolutionary history of enterobactin cheaters in yeasts. This story shows how fungal and bacterial genes can be functionally integrated in the same species for the production of a resource, as well as how eco-evolutionary forces can then separate them as cheaters arise to exploit that resource.

## Materials and Methods

### Construction of *St. bombicola* Deletion Mutants

Genetic manipulations were performed in the *St. bombicola* PYCC 5882 strain, which was obtained from the Portuguese Yeast Culture Collection. Strains used in this study are listed in Dataset S5. All the oligonucleotides used for construction of *St. bombicola* mutants are listed in Dataset S6. The hygromycin-resistance cassette with a *St. bombicola* *GPD* promoter and *S. cerevisiae* *CYC1* terminator was amplified from the previously constructed plasmid PJET-ADH1-HYG (Gonçalves et al. 2018). Genomic DNA of *St. bombicola* PYCC 5882 was isolated and purified using a modified phenol:chloroform extraction method as previously described (Hittinger et al. 2010). For disruption of the *ENB1* and *FRE-TM* genes, two sets of primers were used to amplify  $\sim 1$  kb upstream and  $\sim 1$  kb downstream of their coding sequences with 30 bp overlaps to the hygromycin-resistance cassette. The *ENB1* and *FRE-TM* deletion cassettes were obtained by assembling the upstream and downstream fragments of each gene with the hygromycin-resistance cassette using the NEBuilder HiFi DNA Assembly Master Mix (Catalog# E2621), followed by polymerase chain reaction (PCR) amplifications and cleanup using the QIAquick PCR Purification Kit. Phusion High-Fidelity DNA Polymerase (Catalog# M0530) was used for all the PCR amplifications.

*St. bombicola* was transformed with each deletion cassette using a previously described electroporation protocol (Saerens et al. 2011). The transformants were screened on yeast extract-peptone-dextrose (YPD, 10 g/L yeast extract, 20 g/L peptone, 20 g/L dextrose, pH 7.2) plates supplemented with 650  $\mu\text{g}/\text{mL}$  hygromycin B (HYG, US Biological) and verified using colony PCR and Sanger sequencing.

### Growth and Iron-Binding Assays

*St. bombicola* strains were inoculated from glycerol stocks, which were stored at  $-80^\circ\text{C}$ , to YPD medium and precultured for 3 d at  $30^\circ\text{C}$  in culture tubes. 2% dextrose was used as the carbon source for all cell cultivations. For low-iron cultivations, 1.7 g/L Yeast Nitrogen Base without Amino Acids, Carbohydrates, Ammonium Sulfate, Ferric

Chloride, or Cupric Sulfate (US Biological) was used to make the low-iron synthetic complete (SC) medium ("low-iron medium" in brief) without direct addition of any iron source, although it may inadvertently acquire ambient iron during the medium preparation and cultivation processes. The low-iron medium also consisted of 5 g/L ammonium sulfate, 2 g/L Complete Dropout Mix (US Biological), and 200 nM cupric sulfate. The regular SC medium ("regular medium" in brief) consisted of 200 µg/L (1.2 µM) ferric chloride with all other components kept identical. YP medium contains about 25 µM of iron (Du et al. 2012), which is approximately 20 times of the iron concentration in the regular-iron SC medium. To avoid substantial iron carryover from the YPD precultures, cells were washed twice in deionized water and reinoculated at an initial optical density ( $OD_{600}$ ) of 0.2 in culture tubes with regular- and low-iron media for a second preculture. After 4 d, the cells were again washed and reinoculated at an  $OD_{600}$  of 0.2 into the corresponding media for the growth experiments, which were conducted in 250 mL shake flasks with 50 mL of regular- or low-iron medium at 30 °C.

The chromeazurol S overlay (O-CAS) solution was made with chromeazurol S, ferric chloride hexahydrate, 1,4-piperazinediethanesulfonic acid (free acid), and agarose as described previously (Kominek et al. 2019). Cells of the *St. bombicola* WT and *enb1Δ* strains were precultured in 5 mL YPD medium for 3 d, harvested, and resuspended in 5 mL deionized water. 5 µL of the resulting cell suspension was spotted on the center of 60-mm diameter petri dishes consisting of low-iron SC agarose (1% w/v) and incubated at 30 °C. After 7 d, 6 mL of the O-CAS solution was overlaid onto low-iron SC plates. The plates were sealed with Parafilm and put in the dark at room temperature for another 7 d before pictures were taken on an LED (light-emitting diode) light box.

### Enterobactin Quantification

Supernatants of yeast cultures were harvested by centrifugation at the end of the growth experiments. The amount of enterobactin was quantified using a Shimadzu LCMS8040 by injecting 10 µL of the filtered supernatants onto a Phemonenex Kinetex XB-C18 column (P/N: 00G-4605-E0, 100 Å, 250 × 4.6 mm, 5 µ particle size) held at 50 °C. The mobile phase was a binary gradient of A) water and B) acetonitrile, pumped at 0.7 mL/min. The gradient program was set according to %B using linear gradients between set time points, starting by holding at 5% B for 1 min; then ramping up to 10% B at 5 min and 95% B at 6.5 min; then held at 95% B until 8 min, at which point it was returned to 5% B at 11 min and held at 5% B until the end of the program at 15 min. The column eluent flowed through a photodiode array detector scanning from 250 to 600 nm and into a 2-way switch valve to send it to waste or the mass spectrometer. The mobile phase was diverted to waste from time 0.1 to 3.9 min to aid in keeping the electrospray ionization (ESI) source clean by preventing the buffer salts present in the media from

entering the mass spectrometer. The column eluent was sent to the ESI source from time 3.9 to 15 min.

The dual ion source was set to operate in ESI negative mode, with 2.5 L/min nitrogen nebulizing gas, 15 L/min nitrogen drying gas, desolvation line temperature set to 250 °C, and the heating block temperature set to 400 °C. The mass spectrometer was programmed to collect Q3-scans negative ions from 200 to 1,000  $m/z$  and, for the quantification of enterobactin, three multiple-reaction monitoring (MRM) transitions were acquired: 668→178, CE:53, relative intensity: 100; 668→222, CE:33, relative intensity: 53; and 668→445, CE:21, relative intensity: 22. Argon gas at 230 kPa was used for the MRM fragmentations. The retention time (10.2 min), relative intensities of the three MRM transitions, and a 7-point calibration curve from 125 to 10 µg/mL were determined using an enterobactin standard (Sigma Aldrich #E3910). To minimize carryover, the needle was washed for 10 s before and after each injection. Two blank methanol injections were made between each sample to ensure any carryover enterobactin was below the threshold of detection (~7 µg/mL). As the cell growth varied substantially for the 3 strains grown in different conditions, the concentrations of enterobactin were normalized by the final cell optical density of yeast cultures for fair comparisons.

### Screening for the Presence of ENB1 Homologs

BLASTp analyses in a publicly available genomic assembly of the *St. bombicola* PYCC 5882 strain (GeneBank ID: GCA\_003033785.1) (Gonçalves et al. 2018) were performed using the Enb1 protein sequences from *Saccharomyces cerevisiae* (ScEnb1) as the query. The identified ENB1 ortholog in *St. bombicola* was functionally validated using targeted gene replacement as described above and designated as *StbENB1*. To ascertain whether Enb1-like transporters could be found outside the fungal kingdom, the ScEnb1 amino-acid sequence was used as BLASTp query against the NCBI non-redundant protein sequence (nr) database (supplementary datasets S1 to 1 & S1 to 2, Supplementary Material online). The hits with  $E$ -values  $< 2e-60$  were filtered by removing redundant sequences with  $> 90\%$  similarity using the clustering function of the MMseq2 (Steinegger and Söding 2017). The resulting 1,165 sequences were used to construct a ML phylogeny. We visualized and plotted phylogenetic trees using iTOL (Interactive Tree of Life) v5 (Letunic and Bork 2021). To evaluate the prevalence of ENB1 homologs among fungal genomes, a HMMER sequence similarity search (v3.3, <http://hmmer.org>) was conducted against all the protein-coding sequences pulled out from 1,644 published fungal genome assemblies (Li et al. 2021) using the aligned sequences of ScEnb1 and *StbENB1* as the query. HMMER hits with  $E$ -values  $< 0.05$  are listed in supplementary dataset S3, Supplementary Material online, and protein hits with bit-scores  $> 300$  were retrieved for phylogenetic analyses.

We also identified homologs of Enb1 across the 345 published yeast genome assemblies (Shen et al. 2018;

Kominek et al. 2019) using a separate HMMER search. Protein annotations used for the HMMER search were generated previously by the MAKER genome annotation pipeline v2.31.8 (Holt and Yandell 2011; Shen et al. 2018; Kominek et al. 2019), again using the alignment of ScEnb1 and StbEnb1 sequences as the query. HMMER hits with E-values  $< 0.05$  were listed in supplementary dataset S3, Supplementary Material online, and the 435 hits with bit-scores  $> 300$  were retrieved for constructing a ML phylogeny (Fig. 2). We similarly retrieved Enb1 homologs from the recently published genomes of *W. shivajii* and *St. stellata* (Opulente et al. 2023).

### Phylogenetic Analyses and Topology Tests

Protein sequences of hits from the aforementioned HMMER and BLASTp analyses were retrieved to construct ML trees to infer the phylogenetic relationships of *ENB1* homologs. MAFFT (Multiple Alignment using Fast Fourier Transform) (Katoh and Standley 2013) v7.508 was used to align the sequence with the strategy L-INS-i. Initial inferences of the phylogenies were performed with IQ-TREE (Nguyen et al. 2015) v2.2.0.3 using ModelFinder (Kalyaanamoorthy et al. 2017) with automated model selection based on 1,000 bootstrap pseudoreplicates. The LG + R10, LG + G4, LG + R7, and LG + R10 amino-acid substitution models were selected because they had the lowest Bayesian Information Criterion scores to construct the trees in Figs. 2, 3a, supplementary figs. S1 and S2, Supplementary Material online, respectively. The seven closest relatives of the Enb1 orthologs in filamentous fungi were chosen as outgroups for the Enb1 phylogeny (Fig. 3). To investigate the likelihood of HGT events between the W/S clade and order Saccharomycetales, phylogenetic analyses of Enb1 proteins were repeated with specific constraints, and significance was assessed with AU and wSH topology tests. The constrained tree in Fig. 3b enforced the reciprocal monophyly of the Saccharomycetales and the W/S clade, while the constrained trees in supplementary fig. S4, Supplementary Material online enforced the repositioning of *St. stellata* and *W. versatilis*. The substitution model selected for all the constrained trees was LG + G4.

### Estimating Patterns of Selection

We estimated the ratio of nonsynonymous to synonymous substitution rates (dN/dS) along each branch of the pruned Enb1 protein tree (supplementary fig. S5, Supplementary Material online) using PAML 4 (Phylogenetic Analysis by Maximum Likelihood, version 4) under model 1 (Yang 2007). Branches with very low synonymous substitution rates ( $dS < 0.005$ ) were excluded from the dN/dS analysis because they would lead to artificially high values (supplementary dataset S7, Supplementary Material online).

### Supplementary Materials

Supplementary material is available at *Molecular Biology and Evolution* online.

### Acknowledgments

We thank David J. Krause, Trey K. Sato, and members of the Hittinger and Rokas groups for helpful discussions.

### Author Contributions

L.S. performed all experiments and analyses, except where otherwise noted, and drafted and edited the manuscript. K.T.D. assisted with topology tests. J.F.W. set up the HMMER pipeline and performed the dN/dS analysis. S.D.K. performed enterobactin detection assays. C.G. and M.G. provided reagents and advised on their use. D.A.O., A.L.L., X.Z., and X.X.S. provided genome sequences and annotations. L.S., A.R., and C.T.H. designed and conceived the study. A.R. and C.T.H. secured funding and edited the manuscript. All authors approved the manuscript.

### Funding

This material is based upon work supported in part by the Great Lakes Bioenergy Research Center, U.S. Department of Energy, Office of Science, Biological and Environmental Research Program under Award Number DE-SC0018409; the National Science Foundation (under grant Nos. DBI-2305612 to K.T.D., DEB-2110403 to C.T.H., and DEB-2110404 to A.R.); and the National Institute of Food and Agriculture, United States Department of Agriculture, Hatch project 7005101. C.T.H. is an H. I. Romnes Faculty Fellow, supported by the Vice Chancellor for Research and Graduate Education with funding from the Wisconsin Alumni Research Foundation. Research in the Rokas lab is also supported by the National Institutes of Health/National Institute of Allergy and Infectious Diseases (R01 AI153356), and the Burroughs Wellcome Fund.

### Conflict of Interest

A.R. is a scientific consultant for LifeMine Therapeutics, Inc.

### Data Availability

The data underlying this article are available in the article and in its online supplementary material.

### References

- Ajai-Oyetunde OO, Bradley CA. *Rhizoctonia solani*: taxonomy, population biology and management of rhizoctonia seedling disease of soybean. *Plant Pathol.* 2018;67(1):3–17. <https://doi.org/10.1111/ppa.12733>.
- Ali SS, Asman A, Shao J, Firmansyah AP, Susilo AW, Rosmana A, McMahon P, Junaid M, Guest D, Kheng TY, et al. Draft genome sequence of fastidious pathogen *Ceratobasidium theobromae*, which causes vascular-streak dieback in *Theobroma cacao*. *Fungal Biol Biotechnol.* 2019;6(1):14. <https://doi.org/10.1186/s40694-019-0077-6>.
- Ardon O, Bussey H, Philpott C, Ward DM, Davis-Kaplan S, Verroneau S, Jiang B, Kaplan J. Identification of a *Candida albicans* ferrichrome transporter and its characterization by expression in

*Saccharomyces cerevisiae*. *J Biol Chem*. 2001;276(46):43049–43055. <https://doi.org/10.1074/jbc.M108701200>.

Barber MF, Elde NC. Buried treasure: evolutionary perspectives on microbial iron piracy. *Trends Genet*. 2015;31(11):627–636. <https://doi.org/10.1016/j.tig.2015.09.001>.

Butler G, Kenny C, Fagan A, Kurischko C, Gaillardin C, Wolfe KH. Evolution of the MAT locus and its Ho endonuclease in yeast species. *Proc Natl Acad Sci U S A*. 2004;101(6):1632–1637. <https://doi.org/10.1073/pnas.0304170101>.

Carrano C, Raymond K. Ferric ion sequestering agents. 2. Kinetics and mechanism of iron removal from transferrin by enterobactin and synthetic tricarboxylic acids. *J Am Chem Soc*. 1979;101:18. <https://doi.org/10.1021/ja00512a047>.

De Graeve M, De Maeseneire SL, Roelants SLK, Soetaert W. *Starmerella bombicola*, an industrially relevant, yet fundamentally underexplored yeast. *FEMS Yeast Res*. 2018;18(7):foy072. <https://doi.org/10.1093/femsyr/foy072>.

Dhaoui M, Auchère F, Blaiseau P-L, Lesuisse E, Landoulsi A, Camadro J-M, Haguenauer-Tsapis R, Belgareh-Touzé N. Gex1 is a yeast glutathione exchanger that interferes with pH and redox homeostasis. *MBoC*. 2011;22(12):2054–2067. <https://doi.org/10.1091/mbc.e10-11-0906>.

Dias PJ, Sá-Correia I. The drug:H<sup>+</sup> antiporters of family 2 (DHA2), siderophore transporters (ARN) and glutathione:H<sup>+</sup> antiporters (GEX) have a common evolutionary origin in hemiascomycete yeasts. *BMC Genomics*. 2013;14(1):901. <https://doi.org/10.1186/1471-2164-14-901>.

Diffels JF, Seret M-L, Goffeau A, Baret PV. Heavy metal transporters in Hemiascomycete yeasts. *Biochimie*. 2006;88(11):1639–1649. <https://doi.org/10.1016/j.biochi.2006.08.008>.

Du Y, Cheng W, Li W-F. Expression profiling reveals an unexpected growth-stimulating effect of surplus iron on the yeast *Saccharomyces cerevisiae*. *Mol Cells*. 2012;34(2):127–132. <https://doi.org/10.1007/s10059-012-2242-0>.

Dumas Z, Kümmerli R. Cost of cooperation rules selection for cheats in bacterial metapopulations. *J Evol Biol*. 2012;25(3):473–484. <https://doi.org/10.1111/j.1420-9101.2011.02437.x>.

Furrer JL, Sanders DN, Hook-Barnard IG, McIntosh MA. Export of the siderophore enterobactin in *Escherichia coli*: involvement of a 43 kDa membrane exporter. *Mol Microbiol*. 2002;44(5):1225–1234. <https://doi.org/10.1046/j.1365-2958.2002.02885.x>.

Gilliam M. Identification and roles of non-pathogenic microflora associated with honey bees. *FEMS Microbiol Lett*. 1997;155(1):1–10. [https://doi.org/10.1016/S0378-1097\(97\)00337-6](https://doi.org/10.1016/S0378-1097(97)00337-6).

Gonçalves C, Gonçalves P. Multilayered horizontal operon transfers from bacteria reconstruct a thiamine salvage pathway in yeasts. *Proc Natl Acad Sci USA*. 2019;116(44):22219–22228. <https://doi.org/10.1073/pnas.1909844116>.

Gonçalves P, Gonçalves C, Brito PH, Sampaio JP. The *Wickerhamiella*–*Starmerella* clade—a treasure trove for the study of the evolution of yeast metabolism. *Yeast*. 2020;37(4):313–320. <https://doi.org/10.1002/yea.3463>.

Gonçalves C, Wisecaver JH, Kominek J, Oom MS, Leandro MJ, Shen X-X, Opulente DA, Zhou X, Peris D, Kurtzman CP, et al. Evidence for loss and reacquisition of alcoholic fermentation in a fructophilic yeast lineage. *eLife* 2018;7:e33034. <https://doi.org/10.7554/eLife.33034>.

Griffin AS, West SA, Buckling A. Cooperation and competition in pathogenic bacteria. *Nature*. 2004;430(7003):1024–1027. <https://doi.org/10.1038/nature02744>.

Groenewald M, Hittinger CT, Bensch K, Opulente DA, Shen X-X, Li Y, Liu C, LaBella AL, Zhou X, Limtong S, et al. A genome-informed higher rank classification of the biotechnologically important fungal subphylum Saccharomycotina. *Stud Mycol*. 2023;105(1):1–22. <https://doi.org/10.3114/sim.2023.105.01>.

Haas H, Eisendle M, Turgeon BG. Siderophores in fungal physiology and virulence. *Annu Rev Phytopathol*. 2008;46(1):149–187. <https://doi.org/10.1146/annurev.phyto.45.062806.094338>.

Heymann P, Ernst JF, Winkelmann G. Identification of a fungal triacytlyfusarinine C siderophore transport gene (TAF1) in *Saccharomyces cerevisiae* as a member of the major facilitator superfamily. *Biometals*. 1999;12(4):301–306. <https://doi.org/10.1023/A:1009252118050>.

Heymann P, Ernst JF, Winkelmann G. A gene of the major facilitator superfamily encodes a transporter for enterobactin (Enb1p) in *Saccharomyces cerevisiae*. *Biometals*. 2000a;13(1):65–72. <https://doi.org/10.1023/A:1009250017785>.

Heymann P, Ernst JF, Winkelmann G. Identification and substrate specificity of a ferrichrome-type siderophore transporter (Arn1p) in *Saccharomyces cerevisiae*. *FEMS Microbiol Lett*. 2000b;186(2):221–227. <https://doi.org/10.1111/j.1574-6968.2000.tb09108.x>.

Heymann P, Gerads M, Schaller M, Dromer F, Winkelmann G, Ernst JF. The siderophore iron transporter of *Candida albicans* (Sit1p/Arn1p) mediates uptake of ferrichrome-type siderophores and is required for epithelial invasion. *Infect Immun*. 2002;70(9):5246–5255. <https://doi.org/10.1128/IAI.70.9.5246-5255.2002>.

Hittinger CT, Carroll SB. Gene duplication and the adaptive evolution of a classic genetic switch. *Nature*. 2007;449(7163):677–681. <https://doi.org/10.1038/nature06151>.

Hittinger CT, Gonçalves P, Sampaio JP, Dover J, Johnston M, Rokas A. Remarkably ancient balanced polymorphisms in a multi-locus gene network. *Nature*. 2010;464(7285):54–58. <https://doi.org/10.1038/nature08791>.

Holt C, Yandell M. MAKER2: an annotation pipeline and genome-database management tool for second-generation genome projects. *BMC Bioinformatics*. 2011;12(1):491. <https://doi.org/10.1186/1471-2105-12-491>.

Hurst LD, Pál C, Lercher MJ. The evolutionary dynamics of eukaryotic gene order. *Nat Rev Genet*. 2004;5(4):299–310. <https://doi.org/10.1038/nrg1319>.

James SA, Bond CJ, Stanley R, Ravella SR, Péter G, Dlauchy D, Roberts IN. *Apotrichum terrigenum* sp. nov., a soil-associated yeast found in both the UK and mainland Europe. *Int J Syst Evol Microbiol*. 2016;66(12):5046–5050. <https://doi.org/10.1099/ijsem.0.01467>.

Jiricny N, Diggle SP, West SA, Evans BA, Ballantyne G, Ross-Gillespie A, Griffin AS. Fitness correlates with the extent of cheating in a bacterium. *J Evol Biol*. 2010;23(4):738–747. <https://doi.org/10.1111/j.1420-9101.2010.01939.x>.

Julou T, Mora T, Guillon L, Croquette V, Schalk IJ, Bensimon D, Desprat N. Cell-cell contacts confine public goods diffusion inside *Pseudomonas aeruginosa* clonal microcolonies. *Proc Natl Acad Sci USA*. 2013;110(31):12577–12582. <https://doi.org/10.1073/pnas.1301428110>.

Kalyaanamoorthy S, Minh BQ, Wong TK, von Haeseler A, Jermiin LS. ModelFinder: fast model selection for accurate phylogenetic estimates. *Nat Methods*. 2017;14(6):587. <https://doi.org/10.1038/nmeth.4285>.

Katoh K, Standley DM. MAFFT multiple sequence alignment software version 7: improvements in performance and usability. *Mol Biol Evol*. 2013;30(4):772–780. <https://doi.org/10.1093/molbev/mst010>.

Kellis M, Patterson N, Endrizzi M, Birren B, Lander ES. Sequencing and comparison of yeast species to identify genes and regulatory elements. *Nature*. 2003;423(6937):241–254. <https://doi.org/10.1038/nature01644>.

Kominek J, Doering DT, Opulente DA, Shen X-X, Zhou X, DeVirgilio J, Hulfachor AB, Groenewald M, McGee MA, Karlen SD, et al. Eukaryotic acquisition of a bacterial operon. *Cell*. 2019;176(6):1356–1366.e10. <https://doi.org/10.1016/j.cell.2019.01.034>.

Kondrashov FA, Rogozin IB, Wolf YI, Koonin EV. Selection in the evolution of gene duplications. *Genome Biol*. 2002;3(2):research0008.1. <https://doi.org/10.1186/gb-2002-3-2-research0008>.

Kramer J, Özkan Ö, Kümmerli R. Bacterial siderophores in community and host interactions. *Nature Review Microbiology*. 2020;18(3):152–163. <https://doi.org/10.1038/s41579-019-0284-4>.

Krause DJ, Hittinger CT. Functional divergence in a multi-gene family is a key evolutionary innovation for anaerobic growth in *Saccharomyces cerevisiae*. *Mol Biol Evol*. 2022;39(10):msac202. <https://doi.org/10.1093/molbev/msac202>.

Krause DJ, Kominek J, Opulente DA, Shen X-X, Zhou X, Langdon QK, DeVirgilio J, Hulfachor AB, Kurtzman CP, Rokas A, et al. Functional and evolutionary characterization of a secondary metabolite gene cluster in budding yeasts. *Proc Natl Acad Sci U S A*. 2018;115(43): 11030–11035. <https://doi.org/10.1073/pnas.1806268115>.

Lachance M-A, Starmer WT, Rosa CA, Bowles JM, Barker JSF, Janzen DH. Biogeography of the yeasts of ephemeral flowers and their insects. *FEMS Yeast Res*. 2001;1(1):1–8. [https://doi.org/10.1016/S1567-1356\(00\)00003-9](https://doi.org/10.1016/S1567-1356(00)00003-9).

Lesuisse E, Blaiseau P-L, Dancis A, Camadro J-M. Siderophore uptake and use by the yeast *Saccharomyces cerevisiae*. *Microbiology*. 2001;147(2):289–298. <https://doi.org/10.1099/00221287-147-2-289>.

Lesuisse E, Simon-Casteras M, Labbe P. Siderophore-mediated iron uptake in *Saccharomyces cerevisiae*: the *SIT1* gene encodes a ferrioxamine B permease that belongs to the major facilitator superfamily. *Microbiology*. 1998;144(12):3455–3462. <https://doi.org/10.1099/00221287-144-12-3455>.

Letunic I, Bork P. Interactive Tree Of Life (iTOL) v5: an online tool for phylogenetic tree display and annotation. *Nucleic Acids Res*. 2021;49(W1):W293–W296. <https://doi.org/10.1093/nar/gkab301>.

Li Y, Steenwyk JL, Chang Y, Wang Y, James TY, Stajich JE, Spatafora JW, Groenewald M, Dunn CW, Hittinger CT, et al. A genome-scale phylogeny of the kingdom Fungi. *Curr Biol*. 2021;31(8):1653–1665.e5. <https://doi.org/10.1016/j.cub.2021.01.074>.

Lolas MA, Castro A, Polanco R, Gainza-Cortés F, Ferrada E, Sosnowski MR, Díaz GA. First report of *Eutypa lata* causing dieback of grapevines (*Vitis vinifera*) in Chile. *Plant Disease*. 2020;104(7):2024. <https://doi.org/10.1094/PDIS-12-19-2531-PDN>.

Marcat-Houben M, Gabaldón T. Beyond the whole-genome duplication: phylogenetic evidence for an ancient interspecies hybridization in the baker's yeast lineage. *PLoS Biol*. 2015;13(8):e1002220. <https://doi.org/10.1371/journal.pbio.1002220>.

Nguyen L-T, Schmidt HA, Von Haeseler A, Minh BQ. IQ-TREE: a fast and effective stochastic algorithm for estimating maximum-likelihood phylogenies. *Mol Biol Evol*. 2015;32(1):268–274. <https://doi.org/10.1093/molbev/msu300>.

Niehus R, Picot A, Oliveira NM, Mitri S, Foster KR. The evolution of siderophore production as a competitive trait. *Evolution*. 2017;71(6):1443–1455. <https://doi.org/10.1111/evol.13230>.

Novo M, Bigey F, Beyne E, Galeote V, Gavory F, Mallet S, Cambon B, Legras J-L, Wincker P, Casaregola S, et al. Eukaryote-to-eukaryote gene transfer events revealed by the genome sequence of the wine yeast *Saccharomyces cerevisiae* EC1118. *Proc Natl Acad Sci U S A*. 2009;106(38):16333–16338. <https://doi.org/10.1073/pnas.0904673106>.

Opulente DA, LaBella AL, Harrison M-C, Wolters JF, Liu C, Yonglin L, Kominek J, Steenwyk JL, Stoneman HR, VanDenAvond J, et al. Genomic and ecological factors shaping specialization and generalism across an entire subphylum. *bioRxiv*. <https://doi.org/10.1101/2023.06.19.545611>, last accessed 13 November 2023, preprint: not peer reviewed.

Paysan-Lafosse T, Blum M, Chuguransky S, Grego T, Pinto BL, Salazar GA, Bileshi ML, Bork P, Bridge A, Colwell L, et al. InterPro in 2022. *Nucleic Acids Res*. 2023;51(D1):D418–D427. <https://doi.org/10.1093/nar/gkac993>.

Quaedvlieg W, Kema GHJ, Groenewald JZ, Verkley GJM, Seifbarghi S, Razavi M, Mirzadi Gohari A, Mehrabi R, Crous PW. *Zymoseptoria* gen. nov.: a new genus to accommodate Septoria-like species occurring on graminicolous hosts. *Persoonia*. 2011;26(1):57–69. <https://doi.org/10.3767/003158511X571841>.

Raguzzi F, Lesuisse E, Crichton RR. Iron storage in *Saccharomyces cerevisiae*. *FEBS Lett*. 1988;231(1):253–258. [https://doi.org/10.1016/0014-5793\(88\)80742-7](https://doi.org/10.1016/0014-5793(88)80742-7).

Raymond KN, Dertz EA, Kim SS. Enterobactin: an archetype for microbial iron transport. *Proc Natl Acad Sci U S A*. 2003;100(7): 3584–3588. <https://doi.org/10.1073/pnas.0630018100>.

Saerens KMJ, Saey L, Soetaert W. One-step production of unacetylated sophorolipids by an acetyltransferase negative *Candida bombicola*. *Biotechnol Bioeng*. 2011;108(12):2923–2931. <https://doi.org/10.1002/bit.23248>.

Schiessl KT, Janssen EM-L, Kraemer SM, McNeill K, Ackermann M. Magnitude and mechanism of siderophore-mediated competition at low iron solubility in the *Pseudomonas aeruginosa* pyochelin system. *Front Microbiol*. 2017;8:1964. <https://doi.org/10.3389/fmicb.2017.01964>.

Shen X-X, Opulente DA, Kominek J, Zhou X, Steenwyk JL, Buh KV, Haase MAB, Wisecaver JH, Wang M, Doering DT, et al. Tempo and mode of genome evolution in the budding yeast subphylum. *Cell*. 2018;175(6):1533–1545.e20. <https://doi.org/10.1016/j.cell.2018.10.023>.

Stearman R, Yuan DS, Yamaguchi-Iwai Y, Klausner RD, Dancis A. A permease-oxidase Complex involved in high-affinity iron uptake in yeast. *Science*. 1996;271(5255):1552–1557. <https://doi.org/10.1126/science.271.5255.1552>.

Steinegger M, Söding J. MMseqs2 enables sensitive protein sequence searching for the analysis of massive data sets. *Nat Biotechnol*. 2017;35(11):1026–1028. <https://doi.org/10.1038/nbt.3988>.

Takashima M, Manabe R, Nishimura Y, Endoh R, Ohkuma M, Sriswasdi S, Sugita T, Iwasaki W. Recognition and delineation of yeast genera based on genomic data: Lessons from Trichosporonales. *Fungal Genet Biol*. 2019;130:31–42. <https://doi.org/10.1016/j.fgb.2019.04.013>.

Thomma BPHJ, Van Esse HP, Crous PW, De Wit PJGM. *Cladosporium fulvum* (syn. *Passalora fulva*), a highly specialized plant pathogen as a model for functional studies on plant pathogenic Mycosphaerellaceae. *Mol Plant Pathol*. 2005;6(4):379–393. <https://doi.org/10.1111/j.1364-3703.2005.00292.x>.

Usher KC, Özkan E, Gardner KH, Deisenhofer J. The plug domain of FepA, a TonB-dependent transport protein from *Escherichia coli*, binds its siderophore in the absence of the transmembrane barrel domain. *Proc Natl Acad Sci U S A*. 2001;98(19):10676–10681. <https://doi.org/10.1073/pnas.18135398>.

Vakirlis N, Sarilar V, Drillon G, Fleiss A, Agier N, Meyniel J-P, Blanpain L, Carbone A, Devillers H, Dubois K, et al. Reconstruction of ancestral chromosome architecture and gene repertoire reveals principles of genome evolution in a model yeast genus. *Genome Res*. 2016;26(7):918–932. <https://doi.org/10.1101/gr.204420.116>.

Wang M, Schaefer AL, Dandekar AA, Greenberg EP. Quorum sensing and policing of *Pseudomonas aeruginosa* social cheaters. *Proc Natl Acad Sci U S A*. 2015;112(7):2187–2191. <https://doi.org/10.1073/pnas.1500704112>.

Weigert M, Kümmerli R. The physical boundaries of public goods co-operation between surface-attached bacterial cells. *Proc R Soc B*. 2017;284(1858):20170631. <https://doi.org/10.1098/rspb.2017.0631>.

Yang Z. PAML 4: phylogenetic analysis by maximum likelihood. *Mol Biol Evol*. 2007;24(8):1586–1591. <https://doi.org/10.1093/molbev/msm088>.

Yun C-W, Bauler M, Moore RE, Klebba PE, Philpott CC. The role of the FRE family of plasma membrane reductases in the uptake of siderophore-iron in *Saccharomyces cerevisiae*. *J Biol Chem*. 2001;276(13):10218–10223. <https://doi.org/10.1074/jbc.M010065200>.

Yun C-W, Tiedeman JS, Moore RE, Philpott CC. Siderophore-Iron uptake in *Saccharomyces cerevisiae*: identification of ferrichrome and fusarinine transporters. *J Biol Chem*. 2000;275(21):16354–16359. doi:10.1074/jbc.M001456200.